In-reactor behaviour and economic assessment of enriched gadolinia burnable absorbers

Bolukbasi, Mustafa; Middleburgh, Simon; Lee, Bill

Progress in Nuclear Energy

DOI:
10.1016/j.pnucene.2023.104873

Published: 01/10/2023

Publisher's PDF, also known as Version of record

Progress in Nuclear Energy 164 (2023) 104873

Contents lists available at ScienceDirect

Progress in Nuclear Energy

journal homepage: www.elsevier.com/locate/pnucene

In-reactor behaviour and economic assessment of enriched gadolinia burnable absorbers

M.J. Bolukbasi *, S.C. Middleburgh, W.E. Lee

Nuclear Futures Institute, Bangor University, Bangor, LL57 1UT, UK

ARTICLE INFO

Keywords:
Burnable absorber
Gadolinium oxide
Fuel cycle
Casmo4/Simulate3
Advanced technology fuel

ABSTRACT

The increasing demand for energy and rising energy prices have increased the importance of the efficiency and economic viability of operating nuclear power plants. One approach to improving the reactivity control in such cases is the use of burnable absorbers such as gadolinium oxide (Gd_2O_3). While Gd_2O_3 has proven effective in regulating reactivity in light water reactors, it has certain drawbacks, including the displacement of fissile isotopes from the fuel composition and residual reactivity penalties caused by isotopes other than the main neutron absorbers. In this study, the potential impacts of ^{157}Gd-enriched Gd_2O_3 on the operation, safety, and economy of nuclear power plants were assessed. Fuel cycle analyses were conducted using the advanced nuclear design code system Studsvik CASMO4/SIMULATE3. Several aspects were analysed, including peaking factors, reactivity feedback parameters, power distribution, and shutdown margin. The results of the analysis revealed that by removing the isotopes responsible for residual reactivity from Gd_2O_3, it was possible to achieve the same fuel cycle length with lower uranium enrichment levels, enabling a higher concentration of fissile isotopes and yielding economic benefits without compromising safety.

1. Introduction

In recent years, the rise in energy demand and the rise in energy prices has increased the attractiveness of nuclear energy. In this context, countless studies are being undertaken to further increase the economic efficiency of nuclear power plants (NPPs), without compromising safety. One of the most important methods to achieve this goal is operating the NPP in extended fuel cycle length, reducing the planned outage proportion and therefore increasing capacity factor. However, increased fuel cycle length generally requires the need for higher fuel enrichment (Durazzo et al., 2018) or fuels with higher fissile material (Burns et al., 2020) which makes controlling the reactivity more challenging.

Burnable absorbers (BAs) are of great importance in today's NPPs as they control the reactivity in long fuel cycles, particularly at the beginning of life (BOL) in fresh fuel. BAs prevent excess reactivity during reactor operation, and thus allow a smoother burn-up requiring less reliance on control rod movement (Evans et al., 2022). Additionally, some forms of BA harden the neutron spectrum and reduces the ^{235}U depletion and thus, results in higher fissile ^{239}Pu breeding during reactor operation (Uguru et al., 2020). These fissile ^{239}Pu nuclei provides higher reactivity at the end of the fuel's life (Galahom, 2018).

With gadolinium's high thermal neutron capture cross-section, gadolinium oxide (Gd_2O_3) is one of the most attractive and regularly used BAs. It is used as an integral burnable absorbers (IBA), typically within the limited number of fuel rods in the range of 0.1 wt% to 14 wt% (Papynov et al., 2020; Tran et al., 2017). Since the gadolinium (Gd) isotopes in the outer layers of the fuel pellet capture the neutrons that moderated by the cooling water, the BA isotopes in the inner layers are depleted later (Franceschini and Petrović, 2009). The self-shielding effect results in a suppression of reactivity, but as the Gd isotopes become depleted, the reactivity increases and ultimately reaches the level of reactivity of fuel without the presence of Gd isotopes when the Gd isotopes are almost completely depleted (Tran et al., 2019).

Although Gd_2O_3 provides lower initial reactivity, it has an important disadvantage that limits its performance, thus the performance of the fuel during reactor operation. Natural Gd_2O_3 has 7 stable isotopes in its content, and among these ^{155}Gd and ^{157}Gd are the main neutron-absorbing isotopes with high thermal neutron capture cross-section (see Table 1) (Khoshahval, 2022). As can be seen in, when natural Gd2O3 (n-Gd_2O_3) is used in the fuel composition, after the burning away of ^{155}Gd and ^{157}Gd, the reactivity follows a trend similar to fuel without BA but the isotopes with a low thermal neutron capture cross-section

* Corresponding author.
E-mail address: mbolukbasi@bangor.ac.uk (M.J. Bolukbasi).

https://doi.org/10.1016/j.pnucene.2023.104873
Received 12 January 2023; Received in revised form 18 August 2023; Accepted 25 August 2023
Available online 31 August 2023

Table 1
Natural abundances and thermal absorption cross-sections (at 2200) m/s of natural Gd isotopes (Khoshahval, 2022).

Isotope	Abundance wt.%	σ, barn
Gd-152	0.2	735
Gd-154	2.1	85
Gd-155	14.8	61,100
Gd-156	20.6	1.5
Gd-157	15.65	259,000
Gd-158	24.8	2.2
Gd-160	21.8	0.77

cause reactivity suppression at the later life of the fuel. This phenomenon called the residual reactivity penalty. The increase in the amount of Gd_2O_3 in the fuel composition causes the residual reactivity to increase (Bolukbasi et al., 2021).

Many disadvantages of Gd_2O_3 can be eliminated by enriching it with its most absorbing isotope, ^{157}Gd (Santala et al., 1997). While this enrichment process can eliminate the residual reactivity penalty by removing the isotopes responsible, it also allows for a reduction in the total BA integreted within the fuel to provide the same beginning of life suppression, and thus more fissile material can be loaded into the reactor (Yilmaz, 2005). In addition, the decrease in the Gd_2O_3 content in the fuel composition will reduce the thermal conductivity reduction (Dalle et al., 2013; Qin et al., 2020).

While Santala et al. (1997), suggested that enrichment with ^{157}Gd could be accomplished with conventional techniques (Santala et al., 1997), Renier and Grossbeck (2001), argued that the high cost of these techniques, up to $1,000 per gram of Gd, would make it more expensive than the fuel itself but could be reduced by using new techniques such a plasma separation process (PSP) (Renier and Grossbeck, 2001). Later, Yilmaz (2005), concluded that the cost of the ^{157}Gd enrichment process using PSP costs less than $10 g/$^{157}Gd$ (Yilmaz, 2005).

Bejmer and Seveborn (2004) conducted an in-reactor performance evaluation using enriched Gd_2O_3 (e-Gd_2O_3) enriched with 70 wt% ^{157}Gd in 3-loop PWR. They argued that e-Gd_2O_3 in the reactor core is a more effective burnable absorber (BA) compared to n-Gd_2O_3. It allows loading of higher fissile isotopes when the uranium enrichment amount is kept constant. And they indicated that the effective full power days (EFPDs) can be prolonged due to the elimination of residual reactivity (Bejmer and Seveborn, 2004).

Dalle et al. (2013), investigated the effects of different BA levels in their study using e-Gd_2O_3 enriched with ^{155}Gd. In their study, they stated that e-Gd_2O_3 enriched with ^{155}Gd can obtain more stable reactivity in long cycles compared to n-Gd_2O_3. They also stated that assessment on thermal hydraulic parameters is important (Dalle et al., 2013).

Yilmaz et al. (2006) investigated the effects of the use of different e-Gd_2O_3 fuel models, enriched with ^{155}Gd and ^{157}Gd in different levels, on fuel performance. They stated that since the use of e-Gd_2O_3 reduces the BA concentration in fuel composition the displacement of UO_2 decreases. In this way, the reactivity behaviour provided by the fuel composition containing n-Gd_2O_3 can be achieved with fuel with lower uranium enrichment where e-Gd_2O_3 is used as BA. They also noted that, compared to the total fuel cycle cost, e-Gd_2O_3 could lead to savings of 3.13% in gross and 2.08% net. (Yilmaz et al., 2006).

Campolina et al. (2018), examined the neutronic performance of e-Gd_2O_3 in the PWR Angra-2 reactor fuel assembly. It was determined that fuel cycle cost benefits are bestowed by the low BA loading offered by e-Gd_2O_3, as it facilitates prolonged cycle operation. They estimated that an economic advantage of generating additional power throughout an extended cycle to be $4 million, indicating that a Gd enrichment cost below $371/g could potentially yield savings (Campolina et al., 2018).

Khoshahval (2022), investigated the effective utilization of e-Gd_2O_3 in AP-1000 fuel assemblies examining the various neutronic parameters of the AP-1000 fuel assembly, such as infinite multiplication factor, peak pin power, reactivity swing, and residual binding, at different burnups. The author stated that the reactivity change in the cases involving enriched ^{155}Gd was smoother compared to those involving enriched ^{157}Gd. Based on the findings, it was concluded that e-Gd_2O_3 containing enriched ^{155}Gd and/or ^{157}Gd surpasses natural gadolinium as a burnable poison in terms of reactivity swing and residual binding, without negatively affecting power peaking (Khoshahval, 2022).

Bolukbasi et al. (2021), investigated the reactivity behaviour of e-Gd_2O_3 usage scenarios. In the study, it was noted that increasing the Gd_2O_3 ratio in the fuel composition, and thus the ratio of isotopes with low thermal neutron capture cross-section, escalates the residual reactivity penalty. Moreover, the study revealed that the use of e-Gd_2O_3, which is accepted to be enriched with ^{157}Gd at the rate of one hundred percent, reduces the required amount of BA in the fuel composition and the same reactivity behaviour can be obtained with n-Gd_2O_3. In addition, it was shown that higher reactivity, and therefore higher burn-up, could be obtained at the end of the cycle (EOC), with the possibility of higher fissile isotope loading and the elimination of the residual reactivity penalty (Bolukbasi et al., 2021).

In this study, the possible effects of using e-Gd_2O_3 instead of n-Gd_2O_3 as BA in the reactor operation were examined considering the operational safety and design parameters, such as the moderator temperature coefficient and the shutdown margin, and the economic advantages of using e-Gd_2O_3 were examined.

2. Method

Simulations were performed with Studsvik CASMO4/SIMULATE3 advanced nuclear design code system.

CASMO4, is a burnup calculation software that utilizes a multigroup two-dimensional transport theory approach. The neutron transport equation for individual assemblies or groups of assemblies is solved using a 2D method of characteristics algorithm and generates cross section data for SIMULATE3. SIMULATE3, on the other hand, is an extensively used advanced two-group nodal code for analysing core performance in 3D. This code utilizes the QPANDA neutronics model, which employs fourth-order polynomial representations of the intra-nodal flux distributions in both the fast and thermal neutrons (Bloore, 2013).

A Westinghouse Electric Company standard 3-loop PWR reactor was chosen as a reference NPP to carry out the simulations, and some of the

Table 2
Design parameters and operation limits used in the simulations (DiGiovine and Gheorghiu, 1999; Duke Energy, 2018; U.S.NRC, 1982).

Reactor Type	3-Loop PWR
Coolant inlet temperature at full power (°C)	286.0
Average fuel temperature at full power (K)	820.5
Power Output (MWt/MWe)	2900/965
System pressure (MPa)	15.5
Control rod material	Ag - In – Cd
Number of assemblies	157
Rod array	17 × 17
Assembly pin pitch (cm)	1.26
Fuel pellet radius (cm)	0.410
Number of control rods/guide tube	24/1
Number of BA rods	24
Fuel assembly pitch (cm)	21.50
Fuel assembly height (cm)	365.76
Cladding material	Zircaloy-4
UO_2 fuel density (% of TD)	95
Nuclear Enthalpy Rise Hot Channel Factor ($F_{\Delta H}$)	≤1.66
Heat Flux Hot Channel Factor (F_Q)	≤2.41
Moderator temperature coefficient (pcm/°F)	$-50 \leq$ MTC <0
Shutdown Margin (pcm)	≤ -1770
Electrical power output (MWe)	964
Cycle length (months/days)	18
Effective full power days	508
Refueling outages (days)	40

NPP features in addition to the simulation parameters are given in Table 2. Although some impurities will remain as a result of the enrichment processes, it was assumed that 100% of Gd_2O_3 was enriched with ^{157}Gd in this study in order to observe the full potential of e-Gd_2O_3. The densities of the UO_2/Gd_2O_3 used in the study were calculated with the data obtained from (IAEA, 1995), assuming the enrichment process has no effect on the density of Gd_2O_3. The as-fabricated density of the fuel was then assumed to be 95% of its theoretical density to account for manufactured porosity. In addition, axial blankets were not used in the fuel rods, but a 15.24 cm BA-free area on both the upper and lower parts of the fuel assembly (FA) was preferred for obtaining a flatter axial power distribution.

The two-group cross-section data for approximately 1500 fuel assembly designs were generated using CASMO4. These designs incorporated various levels of ^{235}U enrichment, ranging from 4.40 to 4.95 wt%, as well as different levels of n-Gd_2O_3, ranging from 2 to 10 wt%, along with the corresponding e-Gd_2O_3 levels, which could exhibit similar reactivity behaviour as n-Gd_2O_3. Subsequently, the CMS-Link software package was employed to prepare the necessary library for SIMULATE3.

In the scenario created for the transition from n-Gd_2O_3 to e-Gd_2O_3, it was assumed that the reactor was operating 508 EFPDs in an 18-month fuel cycle, with 64 new fuel assemblies (each has 24 BA rods as in Fig. 1). 29 twice-burned assemblies were discharged in each refueling outage. Fresh fuels were divided into 4 groups to avoid power peaks. The positions of the fresh fuel assemblies and the previous positions of once-burned and twice-burned fuel assemblies in the reactor core are given in Fig. 2.

Approximately 30,000 distinct variations were subjected to testing in SIMULATE3, with the assumption that the fuel model featuring the highest enrichment of ^{235}U could be utilized within the group possessing the least amount of fresh fuel. By doing so, the necessary uranium enrichment and n-Gd_2O_3 levels to achieve the desired effective full power days were ascertained. Subsequently, e-Gd_2O_3 was introduced as a BA for the subsequent cycle and in each simulation, the enrichment level of ^{235}U was decreased to detect the potential reduction in uranium enrichment until reaching the targeted EFPDs, thereby presenting an economic advantage.

The results of numerous simulations revealed that a cycle using n-Gd_2O_3 requires 20 fuel assemblies with 4.75 wt% ^{235}U enrichment and 10.00 wt% BA loading, 16 fuel assemblies with 4.80 wt% ^{235}U enrichment and 10.00 wt% BA loading, 16 fuel assemblies with 4.95 wt% ^{235}U enrichment and 6.00 wt% BA loading, and 12 fuel assemblies with 4.95 wt% ^{235}U enrichment and 4.00 wt% BA loading. Then, simulations to reach 508 EFPDs in the case of e-Gd_2O_3 use showed that the BA content in the fuel composition can be reduced to one-fourth, as well as the required uranium enrichment ratios. Table 3 shows the required BA and uranium enrichment levels for each fuel group for the 508 EFPDs in the n-Gd_2O_3 and e-Gd_2O_3 use scenarios.

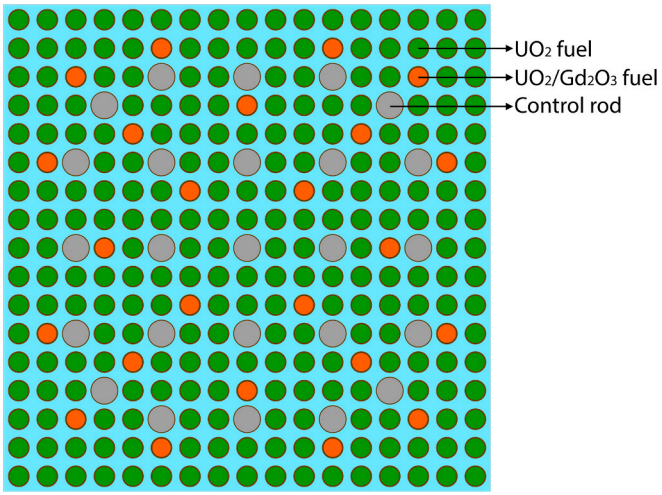

Fig. 1. Fuel assembly design with 24 BA rods (Reda et al., 2020).

It is essential that the fuel compositions meet the reactor's operational and safety limits. Therefore, for all fuel compositions, moderator temperature coefficient, nuclear enthalpy rise hot channel factor, heat flux hot channel factor, isothermal temperature coefficient, uniform doppler coefficient and boron coefficient were examined. In addition, the average axial 2D relative power fraction profile of the fuel core was examined in 12 axial nodes.

All simulations were performed under the conditions of hot full power (HFP), the state that reactor is operating at its full power and the coolant and fuel temperatures are as shown in Table 2, and all control rods out. Additionally, necessary calculations were caried out to determine the change that e-Gd_2O_3 might cause on the shutdown margin. Shutdown margins were calculated with (Eq. (1) (Hiscox, 2018) considering the following situations;

- The difference in reactivity values between HFP and hot zero power (HZP), the state that reactor is operating at zero power and the coolant and fuel temperatures are as shown in Table 2, Δk_1
- The difference in reactivity values between HFP and all control rods are in (ARI), Δk_2
- The difference in reactivity values between ARI and the case if the most effective control rod was not functional, Δk_3

$$SDM = \Delta k_1 + 0.9(\Delta k_2 - \Delta k_3) \quad (1)$$

Considering the unit costs of all components in the front-end of the cycle, the total fuel cost and the fuel cost per MWh were calculated. In addition to uranium purchase, conversion, enrichment, and fabrication costs, the cost of the enrichment process of e-Gd_2O_3 was calculated and included in the cost for the relevant scenario. Unit prices are determined as low, medium, and high to reflect the unexpected changes in unit costs that may emerge in the future. In the calculation of component costs, the method specified by OECD/NEA (OECD/NEA, 1994) was used and component prices were obtained from the literature (U.S. Department of Energy, 2017; Yilmaz, 2005).

Cost calculation methodology, parameter notation, and unit prices are given in Appendix A. However, an example of the formulas used while calculating the component costs is given in (Eq. (2) where X_i is the amount of product processed (kg), f_i is loss factor of operation, P_i is the per unit cost ($), S_i is the escalation rate (%), t is time (year) and, t_i is the base date of monetary unit. In addition, the cost of Gd enrichment was calculated as a separate item and it was assumed that there is no loss in the tails of the ^{157}Gd enrichment process, to simplify the prediction. (Eq. (3) was used to calculate BA costs where M_{Gd} is mass of the required BA (kg) and P_{en} is enrichment cost of Gd ($/gram). It should also be noted that separative work units (SWUs) and fuel enrichment costs are calculated separately for each enrichment level. Lastly, it was assumed that the use of e-Gd_2O_3 does not have any effect on fabrication cost.

$$F_i = X_i \times f_i \times P_i \times (1 + S_i)^{t - t_b} \quad (2)$$

$$F_{e-Gd_2O_3} = M_{Gd} \times P_{en} \times 1000 \quad (3)$$

3. Results and discussion

Critical Boron Concentration (CBC), k_{eff} at BOC, maximum nuclear enthalpy rise hot channel factor and heat flux hot channel factor, burn-up and cycle EFPDs values of the transition cycles, and equilibrium cycles of both n-Gd_2O_3 and e-Gd_2O_3 used scenarios, are given Table 4.

Once the reactor had been initiated, the fuel loading scheme illustrated in Fig. 2 was utilized to simulate the subsequent cycles, with the fuel composition n-Gd_2O_3, depicted in Table 3, from the second cycle. Subsequently, after the tenth cycle, the fuel models containing e-Gd_2O_3 were employed instead of n-Gd_2O_3. The cycle marked as cycle "0" in

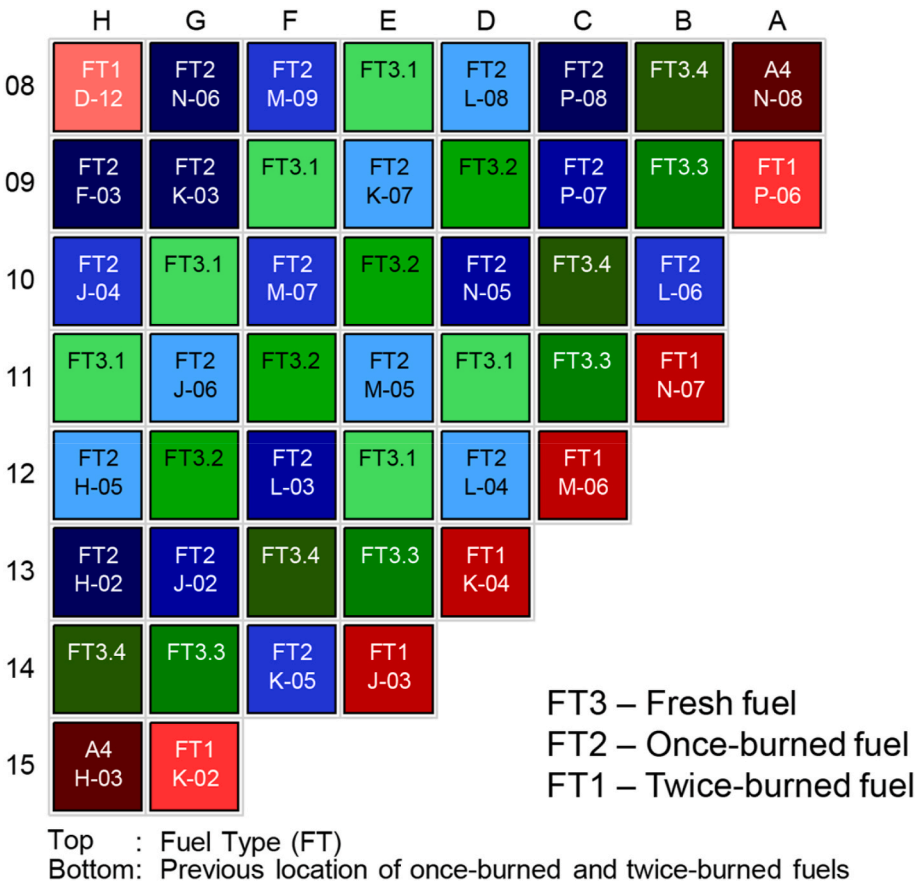

Fig. 2. Fuel loading layout (A to R and 01 to 15 are used to point out the assembly coordinates in the reactor core) (Amjad et al., 2014).

Table 3
Required fuel compositions and number fuel assemblies for 508 EFPDs.

Number of FAs	Fuels with n-Gd_2O_3		Fuels with e-Gd_2O_3		In-core position
	Uranium^{235}U enrichment (wt. %)	BA level (wt. %)	Uranium^{235}U enrichment (wt. %)	BA level (wt. %)	
20	4.75	10.0	4.59	2.5	FT3.1
16	4.80	10.0	4.64	2.5	FT3.2
16	4.95	6.0	4.79	1.5	FT3.3
12	4.95	4.0	4.79	1.0	FT3.4

Table 4 was considered the final cycle in which n-Gd_2O_3 was used as the BA. Starting from cycle 1, e-Gd_2O_3 employed as BA, given that the study focuses on an operational reactor that uses n-Gd_2O_3 considered.

As can be seen in Table 4, the equilibrium cycle has been reached in the case of using e-Gd_2O_3 as of the 4th cycle. The use of e-Gd_2O_3 resulted in an increase of ~1.4% of the required Critical Boron Concentration at the beginning of the cycle, and an increase of about 27% in the middle of the cycle when comparing equilibrium cycles. On the other hand, there is an increase in k_{eff} values at BOC by ~300 pcm. Moreover, when the maximum nuclear enthalpy rise hot channel factor and heat flux hot channel factor values are examined for each cycle, it is seen that the use of e-Gd_2O_3 increases the nuclear enthalpy rise hot channel factor and heat flux hot channel factor, within the reactor design and operation

Table 4
Equilibrium and transition cycles' parameters.

Cycle No.	Cycle Definition	CBC- BOC (ppm)	CBC at 10 GWd/MTU (ppm)	K_{eff}- BOC	Maximum $F_{\Delta H}$	Maximum F_Q	Cycle Burn-up (GWd/MTU)	Cycle EFPDs
−1	n-Gd_2O_3 equilibrium cycle	1,267.7	745.7	1.07886	1.608	1.887	20.187	507.6
0	n-Gd_2O_3 equilibrium cycle	1,267.8	745.7	1.07886	1.608	1.888	20.188	507.6
1	e-Gd_2O_3 transition cycle first feed	1,300.4	968.8	1.08160	1.627	1.910	20.261	510.8
2	e-Gd_2O_3 transition cycle second feed	1,285.7	947.9	1.08179	1.634	1.931	20.099	508.1
3	e-Gd_2O_3 transition cycle third feed	1,286.5	947.3	1.08191	1.635	1.926	20.077	508.1
4*	e-Gd_2O_3 equilibrium cycle	1,285.8	947.1	1.08187	1.635	1.927	20.074	508.0
5	e-Gd_2O_3	1,286.0	947.0	1.08188	1.635	1.927	20.074	508.0
6	e-Gd_2O_3	1,286.0	947.0	1.08188	1.635	1.927	20.074	508.0

safety limits, by about ~1.7% and ~2.0%, respectively due to differences in BA depletion rates.

In Fig. 3, the moderator temperature coefficient, isothermal temperature coefficient, uniform doppler coefficient, and boron coefficient curves of both n-Gd_2O_3 (Fig. 3a) and e-Gd_2O_3 (Fig. 3b) equilibrium cycles are given.

When Fig. 3 is examined, no noticeable change is observed in the uniform doppler coefficient and boron coefficient between n-Gd_2O_3 and e-Gd_2O_3 equilibrium cycles, while a decrease of ~2 pcm/°F was observed in the moderator temperature coefficient and Isothermal Temperature Coefficient values in the first half of the e-Gd_2O_3 equilibrium cycle compared to n-Gd_2O_3 equilibrium cycle.

Table 5 shows the beginning and end of the cycle shutdown margins of the equilibrium cycles of n-Gd_2O_3 and e-Gd_2O_3. As seen in Table 5, although the use of e-Gd_2O_3 causes a relative difference in the shutdown margin (3 pcm for beginning of the cycle and 40 pcm for end of the cycle), it can be said that the use of e-Gd_2O_3 does not have a notable effect on the shutdown margin.

Average axial relative power distribution was examined to determine the change caused by the use of e-Gd_2O_3 on the axial power profile. Fig. 4 shows the average axial 2D relative power distribution graphs of n-Gd_2O_3 and e-Gd_2O_3 equilibrium cycles at beginning and end of the cycle. Examination of Fig. 4 shows that the use of e-Gd_2O_3 did not result in substantial alterations to the average axial relative power distribution. A deviation of ±2% is observed at the beginning of the cycle when results are compared. However, at the end of the cycle, reductions of up to 5% occur in the lower half of the fuel assemblies, while increases of up to 7% are observed in the upper half. These alterations can be attributed to two factors: the higher neutron flux experienced at the bottom of the reactor due to the upward movement of the coolant from that region and the faster depletion rate of ^{157}Gd compared to ^{155}Gd.

The assembly-wise 2D relative power fraction changes resulting from the use of e-Gd_2O_3 were analysed. Fig. 5 presents the 2D relative power fraction comparisons for equilibrium cycles of both n-Gd_2O_3 and e-Gd_2O_3 at the beginning and end of the cycles. Upon examination of Fig. 5, it can be observed that the use of e-Gd_2O_3 causes a change of up to ±0.04 on some once-burned and twice-burned fuel assemblies in terms of 2D relative power fraction at beginning and end of the cycle.

Both n-Gd_2O_3 and e-Gd_2O_3 equilibrium cycles were evaluated economically. As mentioned in the method section, both the fuel loading costs for the cycle and the levelized cost of electricity of the front end of the cycle ($LCOE_{front\text{-}end}$) were evaluated for equilibrium cycles. While the low, nominal, and high costs calculated for both types of BA usage scenarios are given in Table 6, the costs of each component are given as low, nominal, and high in Table A1. As it can be seen when Table 6 is examined, the nominal fuel loading cost of n-Gd_2O_3 is approximately

Table 5
Shutdown margin of n-Gd_2O_3 and e-Gd_2O_3 equilibrium cycles.

Fuel Type	BOC (pcm)	EOC (pcm)
n-Gd_2O_3	−3,734	−2,324
e-Gd_2O_3	−3,737	−2,264

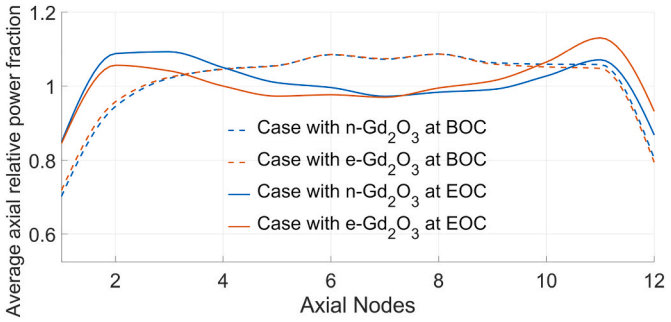

Fig. 4. Average axial relative power distribution curves of n-Gd_2O_3 and e-Gd_2O_3 equilibrium cycles.

$87.48 million per cycle while it is approximately $85.71 million per cycle in the e-Gd_2O_3 usage scenario, and the use of e-Gd_2O_3 provides a saving of approximately $1.77 million when considering nominal prices (varying between $1.06 million to $3.98 million, depending on fluctuation in prices considered).

The use of e-Gd_2O_3 increases the total amount of uranium to be loaded into the reactor core, but when Table A1 is examined, it is seen that the purchase and enrichment costs of uranium, which are the most expensive items of fuel loading cost, decrease. This is because the use of e-Gd_2O_3 requires lower enrichment levels and therefore lower enrichment costs and requires a lower amount of natural uranium feed for the enrichment process. In addition, considering the nominal price, the cost of ^{157}Gd enrichment is approximately $0.55 million (ranging from $0.36 million to $0.84 million depending on the fluctuation in prices), and despite the additional costs of ^{157}Gd enrichment, the use of e-Gd_2O_3 significantly reduces the total cost.

In Table 6, the financial benefit of e-Gd_2O_3 is portrayed, relying on the ^{157}Gd enrichment cost obtained from existing literature data. However, the actual cost of the Gd enrichment process still holds uncertainties. For e-Gd_2O_3 to be considered economically viable, it is imperative that the enrichment cost of ^{157}Gd stays below a predefined threshold.

Fig. 6 summarizes the impact of an increase or decrease in the cost of

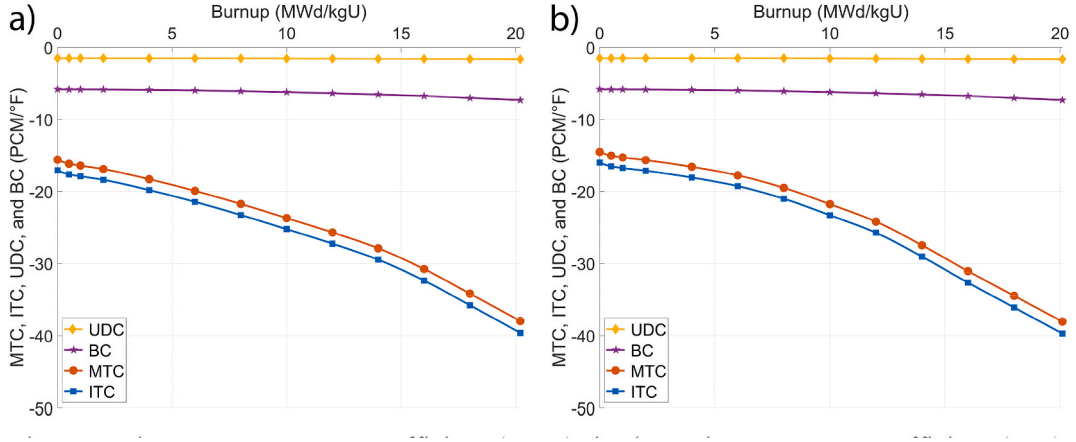

Fig. 3. Moderator temperature coefficient (MTC), isothermal temperature coefficient (ITC), uniform doppler coefficient (UDC), and boron coefficient (BC) curves of (a) n-Gd_2O_3 equilibrium cycle and (b) e-Gd_2O_3 equilibrium cycle.

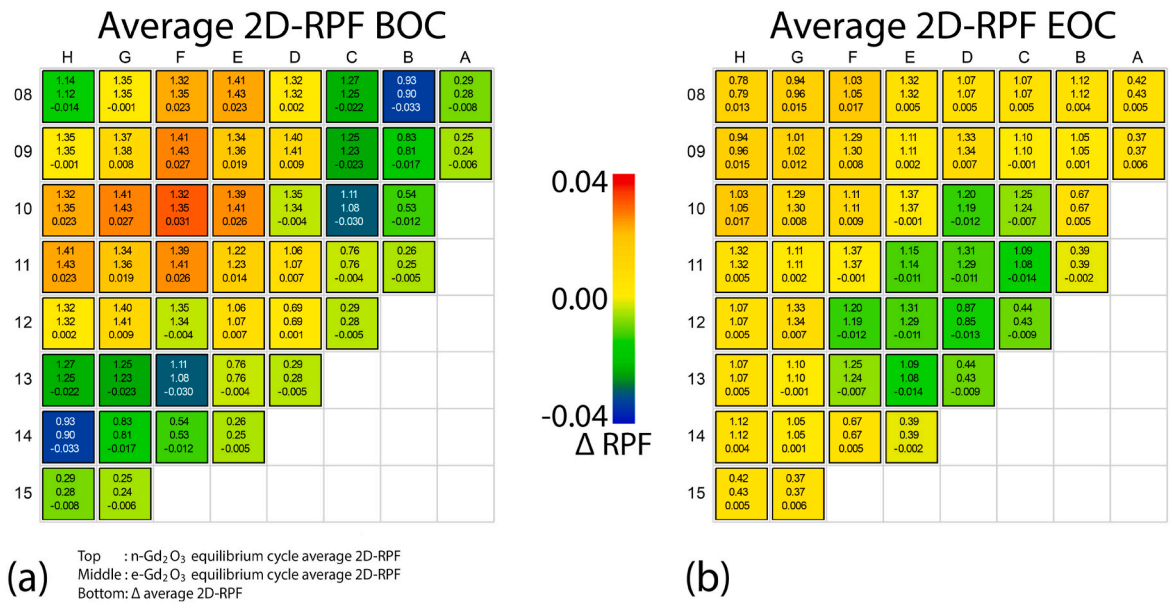

Fig. 5. Assembly-wise average 2D relative power fraction prolife of n-Gd_2O_3 and e-Gd_2O_3 equilibrium cycles at BOC (a) and EOC (b).

Table 6
Fuel loading costs of n-Gd_2O_3 and e-Gd_2O_3 for equilibrium cycles.

	Low ($M)	Nominal ($M)	High ($M)
n-Gd_2O_3	~50.97	~87.48	~180.20
e-Gd_2O_3	~49.9	~85.71	~176.22
Difference	~1.06	~1.77	~3.98

^{157}Gd enrichment on the financial profit to be obtained from the use of e-Gd_2O_3 for low, nominal, and high costs of uranium purchase, conversion, enrichment, fabrication scenarios. When analysing the results with respect to the nominal uranium cost, a crucial point emerges: at an approximate ^{157}Gd enrichment cost of $42 per gram, the profit attained through reduced uranium enrichment becomes entirely offset by the expenses incurred for ^{157}Gd enrichment. Consequently, no net financial gain is achieved. To achieve economic profitability, the enrichment cost of ^{157}Gd must remain below certain levels, depending on the uranium fuel cost scenario. Under the nominal uranium fuel cost scenario, the cost should stay below $42/g. For the low uranium fuel cost scenario, the cost should be kept below $25.6/g. In the case of the high-cost uranium scenario, the enrichment cost must remain below $87.1/g.

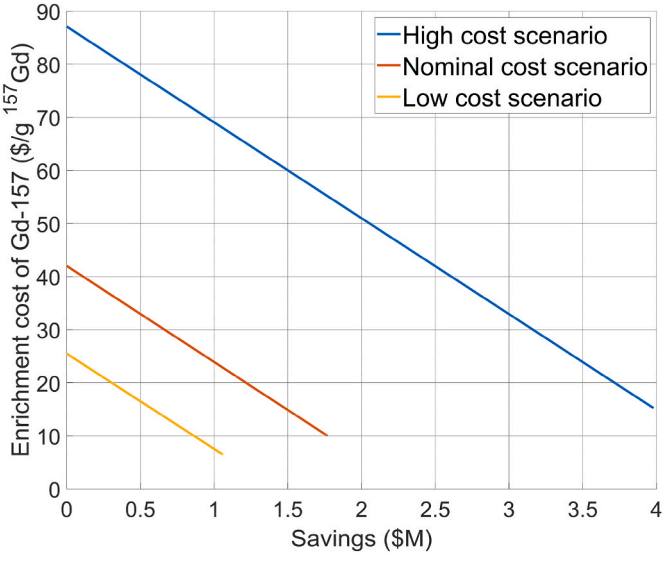

Fig. 6. Changes in savings based on variations in ^{157}Gd enrichment costs, taking into account scenarios with low, nominal, and high front-end unit prices.

The findings highlight the critical importance of controlling the cost of ^{157}Gd enrichment when utilizing e-Gd_2O_3. By having the ^{157}Gd enrichment cost below the specified values, the prospects for achieving a positive economic outcome are significantly enhanced, making the use of e-Gd_2O_3 a more profitable option in the long term.

On the other hand, LCOE of front-end were evaluated for equilibrium cycles in n-Gd_2O_3 and e-Gd_2O_3 usage scenarios. Table 7 shows the $LCOE_{Front\text{-}end}$ costs of n-Gd_2O_3 and e-Gd_2O_3 equilibrium cycles. Considering the nominal prices, the fuel cost per MWh of using n-G_2O_3 is approximately $7.44, while the use of e-Gd_2O_3 provides a savings of approximately $0.15, and this value varies between ~$0.09 and ~$0.34 depending on the fluctuations in prices.

The cost analyses clearly show that the use of e-Gd_2O_3 makes a significant contribution to reducing the total cost, and fuel cost per MWh, despite the additional ^{157}Gd enrichment cost it will bring. For a NPP halfway through its 60-years life, it can be assumed that it will yield savings of more than $28 million in the last half of its service life and have behaviour that could be considered advantageous to safety.

4. Conclusions

The potential in-core behaviour of Gd_2O_3, enriched with ^{157}Gd isotopes, was evaluated. The required uranium enrichment level with the use of e-Gd_2O_3 compared to n-Gd_2O_3 was determined. Also, some of the most important safety parameters such as heat flux hot channel factor, nuclear enthalpy rise hot channel factor, moderator temperature coefficient, isothermal temperature coefficient, critical boron concentration, boron coefficient, uniform doppler coefficient, PRF and shutdown margin were evaluated as well as the economic benefits of e-Gd_2O_3 usage on fuel loading cost and fuel cost per MWh electricity production

Table 7
$LCOE_{Front\text{-}end}$ costs of n-Gd_2O_3 and e-Gd_2O_3 for equilibrium cycles.

	Low ($/MWh)	Nominal ($/MWh)	High ($/MWh)
n-Gd_2O_3	~4.34	~7.44	~15.33
e-Gd_2O_3	~4.24	~7.29	~14.99
Difference	~0.09	~0.15	~0.34

within the fuel cycle.

Because of discharged Gd isotopes with a low thermal neutron cross-section in fuel composition, the use of e-Gd_2O_3 can reduce residual reactivity (Renier and Grossbeck, 2001), allows to load increased the amount of uranium fuel (Yilmaz et al., 2006), thereby targeted EFPDs can be achieved with less ^{235}U enrichment than required by the use of n-Gd_2O_3

Due to the inclusion of e-Gd_2O_3 in the fuel composition, discharged Gd isotopes with a low thermal neutron cross-section can be utilized, resulting in a reduction of residual reactivity (Renier and Grossbeck, 2001). By employing e-Gd_2O_3, it becomes possible to load an increased amount of uranium fuel (Yilmaz et al., 2006), thereby achieving the desired effective full power days (EFPDs) with a lower ^{235}U enrichment requirement compared to the use of n-Gd_2O_3. This allows for a more efficient utilization of uranium resources.

The introduction of e-Gd_2O_3 does not give rise to any adverse effects on critical parameters crucial to safe and reliable operation, such as the heat flux hot channel factor, nuclear enthalpy rise hot channel factor, moderator temperature coefficient, isothermal temperature coefficient, uniform Doppler coefficient, and boron coefficient. Thus, the addition of e-Gd_2O_3 maintains the integrity of these parameters.

Furthermore, the utilization of e-Gd_2O_3 does not exhibit any detectable negative impact on the shutdown margin, which is a critical safety parameter for reactors. This confirms that e-Gd_2O_3 can be employed without compromising the safety.

In terms of the assembly-wise average 2D relative power fraction and average axial relative power distribution, the use of e-Gd_2O_3 does not yield any significant effects. This implies that e-Gd_2O_3 has no substantial influence on the power distribution within the reactor assembly, further solidifying its suitability for practical implementation. Nevertheless, in the lower half of the fuel assemblies, reductions of up to 5% are experienced, whereas increases of up to 7% are observed in the upper half.

Moreover, incorporating e-Gd_2O_3 provides significant cost savings of approximately $1.77 million considering nominal prices compared to n-Gd_2O_3. Although, the additional cost of enriching the ^{157}Gd isotope, the reduction in displaced uranium in fuel composition allows for a lower uranium enrichment requirement. Therefore, the utilization of e-Gd_2O_3 proves to be economically advantageous while maintaining the desired operational efficiency.

Considering the nature of Gd_2O_3, other PWR systems are predicted to follow a similar trend. Future studies should consider that better results can be achieved with a better optimized fuel assembly and reactor core design. In addition, the effect of using e-Gd_2O_3 on thermal properties should be investigated. Additionally, the changes in delayed neutron fraction should also be investigated as it is an important parameter to ensure safety.

Declaration of competing interest

The authors declare that they have no known competing financial interests or personal relationships that could have appeared to influence the work reported in this paper.

Data availability

No data was used for the research described in the article.

Acknowledgements

The authors would like to express their gratitude to the Turkish Republic's Ministry of National Education. SCM and WEL are funded through the Sêr Cymru II programme by Welsh European Funding Office (WEFO) under the European Development Fund (ERDF).

Appendix A

Table A1
Approximate fuel cost of each cycle

	Fuel loading cost of n-Gd_2O_3			Fuel loading cost of e-Gd_2O_3		
	Low	Nominal	High	Low	Nominal	High
Cost of uranium ($M)	12.394	31.316	107.856	12.039	30.419	104.768
Cost of conversion ($M)	2.394	4.788	6.998	2.326	4.651	6.798
Cost of enrichment ($M)	27.516	36.31	43.686	26.464	34.921	42.014
Cost of fabrication ($M)	8.665	15.069	21.661	8.72	15.165	21.799
Cost Of^{157}Gd enrichment ($M)	0	0	0	0.36	0.55	0.84
Cost of total fuel loading ($M)	50.969	87.483	180.201	49.908	85.71	176.223
Savings ($M)				1.06	1.77	3.98

Table A2
Parameter notation for fuel cost calculations. Where:

Time	t
Base date of monetary unit	t_b
Date of fuel loading	t_c
Mass of uranium feed (kg)	M_f
Mass of uranium charged in reactor (kg)	M_p
Mass of uranium in the tails (kg)	M_t
Fraction of^{235}U in the uranium feed	e_f (0.711%)
Fraction of^{235}U charged in reactor	e_p
Fraction of^{235}U in the tails	e_t
Conversion factor from kg U to lb U_3O_8 (a lb U_3O_8 per kg U)–>	a (2.6)
Total component cost	F_i
Unit cost	P_i
Escalation rate	s_i
Material losses	l_i
Total loss factor	f_i

(*continued on next page*)

Table A2 (*continued*)

Lead or lag time	t_i
Power output (MWe)	P_e (964)

Where:

i = 1 Uranium purchaseP_1 = Monetary units per lb U_3O_8

i = 2 ConversionP_2 = Monetary units per kg U

i = 3 EnrichmentP_3 = Monetary units per SWU

i = 4 FabricationP_4 = Monetary units per kgU

Equations used for cost of uranium (Eq. (A1)), conversion (Eq. (A5)), enrichment (Eq. (A7)), fabrication (Eq. (A12)) and the LCOE (Eq. (A15)) are as follows (OECD/NEA, 1994).

Cost of uranium

$$F_1 = M_f \times a \times f_1 \times P_1 \times (1 + S_1)^{t-t_b} \tag{A1}$$

where:

$$M_f = \frac{e_p - e_t}{e_f - e_t} \times M_p \tag{A2}$$

$$f_1 = (1 + l_2) \times (1 + l_3) \times (1 + l_4) \tag{A3}$$

From all front-end components

$$t = t_c - t_i \tag{A4}$$

Cost of conversion

$$F_2 = M_f \times f_2 \times P_2 \times (1 + S_2)^{t-t_b} \tag{A5}$$

where:

$$f_2 = (1 + l_2) \times (1 + l_3) \times (1 + l_4) \tag{Eq. A6}$$

Cost of enrichment

$$F_3 = SWU \times f_3 \times P_3 \times (1 + S_3)^{t-t_b} \tag{A7}$$

where:

$$SWU = M_p V_p + M_t V_t - M_f V_f \tag{A8}$$

$$M_t = M_f - M_p \tag{A9}$$

x is a subscript for f, p or t

$$V_x = (2e_x - 1) \times \ln \frac{e_x}{(1 - e_x)} \tag{A10}$$

$$f_3 = (1 + l_3) \times (1 + l_4) \tag{A11}$$

Cost of fabrication

$$F_4 = M_p \times f_4 \times P_4 \times (1 + S_4)^{t-t_b} \tag{A12}$$

where:

$$f_4 = (1 + l4) \tag{A13}$$

Total cost of fuel

$$Total\ fuel\ cost = \sum_i F_i \tag{A14}$$

$LCOE_{Front\text{-}end}$

$$LCOE_{Front-end} = \frac{\sum_i F_i}{EFPD * 24 * P_e} \tag{A15}$$

Unit prices used for fuel cost calculation are shown in Table A3.

Table A3
Unit prices for each component (U.S. Department of Energy, 2017; Yilmaz, 2005)

Type of component	Unit Prices		
	Low	Nominal	High
uranium $/lb U_3O_8	13.1	33.1	114
conversion $/kg	6.5	13	19
Uranium enrichment $/SWU	97	128	154
fabrication $/kg	230	400	575
^{157}Gd enrichment $/g[a]	6.48	10	15.25

[a] Low unit costs were obtained by assuming that the nominal cost regularly increased and decreased by average USA escalation rate in the period from the year it was stated in the literature (Yilmaz, 2005) to 2022.

Fuel cycle data used for fuel cost calculation are shown in Table A4.

Table A4
Fuel cycle data (Forsberg, 2011; OECD/NEA, 1994; World Nuclear Association, 2021)

Lead time of uranium purchase	24 months
Lead time of conversion	18 months
Lead time of Uranium enrichment	12 months
Lead time of fabrication	6 months
Material loss during conversion (%)	0.2
Material loss during enrichment (%)	0.2
Material loss during fabrication (%)	0.2
Tails assay (%)	0.25
Escalation rate	2.46

References

Amjad, N., Hidekazu, Y., Ming, Y., 2014. Burnup study of 18 months and 16/20 months cycle AP1000 cores using CASMO4E and SIMULATE-3 codes. Nucl. Saf. Simul. 5.

Bejmer, K.H., Seveborn, O., 2004. Enriched gadolinium as burnable absorber for PWR. In: Proceedings of the PHYSOR The Physics of Fuel Cycles and Advanced Nuclear Systems - Global Developments, p. 18. ISSN: 1098-6596. arXiv: arXiv:1011.1669v3.

Bloore, D.A., 2013. Reactor Physics Assessment Of Thick Silicon Carbide Clad Pwr Fuels. Massachusetts Institute Of Technology.

Bolukbasi, M.J., Middleburgh, S.C., Dahlfors, M., Lee, W.E., 2021. Performance and economic assessment of enriched gadolinia burnable absorbers. Prog. Nucl. Energy 137, 103752. https://doi.org/10.1016/j.pnucene.2021.103752.

Burns, J.R., Hernandez, R., Terrani, K.A., Nelson, A.T., Brown, N.R., 2020. Reactor and fuel cycle performance of light water reactor fuel with 235U enrichments above 5. Ann. Nucl. Energy 142, 107423. https://doi.org/10.1016/j.anucene.2020.107423.

Campolina, D., Faria, E.F., Santos, A.A.C., Vasconcelos, V., Franco, M.P.V., Dias, M.S., Mattos, J.R.L., 2018. Parametric study of enriched gadolinium in burnable neutron poison fuel rods for Angra-2. Ann. Nucl. Energy 118, 375–380. https://doi.org/10.1016/j.anucene.2018.04.025.

Dalle, H.M., Mattos, J.R.L. de, Dias, M.S., 2013. Enriched gadolinium burnable poison for PWR fuel – Monte Carlo burnup simulations of reactivity. In: Current Research in Nuclear Reactor Technology in Brazil and Worldwide. https://doi.org/10.5772/53381.

DiGiovine, A.S., Gheorghiu, H.-N.M., 1999. Generic CMS PWR Equilibrium Model Revision 3.

Duke Energy, 2018. Harris Nuclear Power Plant Core Operating Limits Report.

Durazzo, M., Freitas, A.C., Sansone, A.E.S., Ferreira, N.A.M., de Carvalho, E.F.U., Riella, H.G., Leal Neto, R.M., 2018. Sintering behavior of UO2–Er2O3 mixed fuel. J. Nucl. Mater. 510, 603–612. https://doi.org/10.1016/j.jnucmat.2018.08.051.

Evans, J.A., DeHart, M.D., Weaver, K.D., Keiser, D.D., 2022. Burnable absorbers in nuclear reactors – a review. Nucl. Eng. Des. 391, 111726 https://doi.org/10.1016/J.NUCENGDES.2022.111726.

Forsberg, C.W., 2011. The Future of the Nuclear Fuel Cycle. MIT.

Franceschini, F., Petrović, B., 2009. Fuel with advanced burnable absorbers design for the IRIS reactor core: combined Erbia and IFBA. Ann. Nucl. Energy 36, 1201–1207. https://doi.org/10.1016/j.anucene.2009.04.005.

Galahom, A., 2018. Simulate the effect of integral burnable absorber on the neutronic characteristics of a PWR assembly. Nucl. Energy Technol. 4, 287–293. https://doi.org/10.3897/nucet.4.30379.

Hiscox, B., 2018. Analysis and Optimization of a New Accident Tolerant Fuel Called Fuel-In-Fibers. Massachusetts Institute of Technology.

IAEA, 1995. Characteristics and Use of Urania-Gadolinia Fuels 1–191.

Khoshahval, F., 2022. The effect of enriched gadolinia and its concentrations on the neutronic parameters of AP-1000 fuel assembly. Radiat. Phys. Chem. 195, 110086 https://doi.org/10.1016/J.RADPHYSCHEM.2022.110086.

OECD/NEA, 1994. The Economics of the Nuclear Fuel Cycle. Nuclear Energy Agency, Organisation for Economic Co-Operation and Development.

Papynov, E.K., Shichalin, O.O., Belov, A.A., Portnyagin, A.S., Buravlev, I.Y., Mayorov, V. Y., Sukhorada, A.E., Gridasova, E.A., Nomerovskiy, A.D., Glavinskaya, V.O., Tananaev, I.G., Sergienko, V.I., 2020. Spark plasma sintering of UO2 fuel composite with Gd2O3 integral fuel burnable absorber. Nucl. Eng. Technol. 52, 1756–1763. https://doi.org/10.1016/j.net.2020.01.032.

Qin, M.J., Middleburgh, S.C., Cooper, M.W.D., Rushton, M.J.D., Puide, M., Kuo, E.Y., Grimes, R.W., Lumpkin, G.R., 2020. Thermal conductivity variation in uranium dioxide with gadolinia additions. J. Nucl. Mater. 540, 152258 https://doi.org/10.1016/j.jnucmat.2020.152258.

Reda, S.M., Mustafa, S.S., Elkhawas, N.A., 2020. Investigating the Performance and safety features of Pressurized water reactors using the burnable poisons. Ann. Nucl. Energy 141, 107354. https://doi.org/10.1016/j.anucene.2020.107354.

Renier, J.-P.A., Grossbeck, M.L., 2001. Development of Improved Burnable Poisons for Commerical Nuclear Power Reactors.

Santala, M.I.K., Daavittila, A.S., Lauranto, H.M., Salomaa, R.R.E., 1997. Odd-isotope enrichment studies of Gd by double resonance laser-ionization for the production of burnable nuclear reactor poison. Appl. Phys. B Laser Opt. 64, 339–347. https://doi.org/10.1007/s003400050182.

Tran, H.N., Hoang, H.T.P., Liem, P.H., 2017. Feasibility of using Gd2O3 particles in VVER-1000 fuel assembly for controlling excess reactivity. Energy Proc. 131, 29–36. https://doi.org/10.1016/j.egypro.2017.09.442.

Tran, H.N., Hoang, V.K., Liem, P.H., Hoang, H.T.P., 2019. Neutronics design of VVER-1000 fuel assembly with burnable poison particles. Nucl. Eng. Technol. 51, 1729–1737. https://doi.org/10.1016/J.NET.2019.05.026.

U.S. Department of Energy, 2017. Advanced Fuel Cycle Cost Basis –, 2017 Edition.

U.S.NRC, 1982. Technical Specifications, Virgil C. Summer Nuclear Station.

Uguru, E.H., Sani, S.F.A., Khandaker, M.U., Rabir, M.H., Karim, J.A., 2020. A comparative study on the impact of Gd2O3 burnable neutron absorber in UO2 and (U, Th)O2 fuels. Nucl. Eng. Technol. 52, 1099–1109. https://doi.org/10.1016/j.net.2019.11.010.

World Nuclear Association, 2021. HARRIS 1 Operating details [WWW Document]. URL. https://www.world-nuclear.org/reactor/default.aspx/HARRIS-1.

Yilmaz, S., 2005. Multi Level Optimization of Burnable Poison Utilization for Advanced PWR Fuel Management. The Pennsylvania State University.

Yilmaz, S., Ivanov, K., Levine, S., Mahgerefteh, M., 2006. Development of enriched Gd-155 and Gd-157 burnable poison designs for a PWR core. Ann. Nucl. Energy 33, 439–445. https://doi.org/10.1016/j.anucene.2005.11.011.